Available online at www.sciencedirect.com
ScienceDirect
Catalysis Today 131 (2008) 55–60
CATALYSIS TODAY
www.elsevier.com/locate/cattod

Structural and catalytic characterization of nanosized mesoporous aluminosilicates synthesized via a novel two-step route

Shang-Ru Zhai [a,b], Il Kim [b], Chang-Sik Ha [b,*]

[a] *Faculty of Chemical Engineering and Materials, Dalian Polytechnic University, Dalian 116034, China*
[b] *Department of Polymer Science and Engineering, Pusan National University, Busan 609-705, Republic of Korea*

Available online 26 November 2007

Abstract

Nanosized Al-containing mesostructures with a narrow grain size distribution and high aluminum content (Si/Al $\geq$ 5) have been facilely prepared via a novel two-step synthetic process, in which the pre-hydrolysis and afterward fast-assembly of inorganic species can be conveniently promoted by acidic aluminum salt and basic catalyst, respectively. Meanwhile, nonionic polyethylene glycol (PEG-4000) added in the synthesis can effectively regulate the grain size and distribution through hydrogen-bonding blocking. Along with high density of acidic sites, the interesting morphology consisted of slight aggregation of nanoparticles with AlMCM-41 structure and thereby formation of a second broader porous system in these interparticle voids may be responsible for its superior activity in the bulky hydrocarbon cracking reactions; i.e. not only good catalytic behavior to the transformation of 1,3,5-triisopropylbenzene even at the lowest temperature tested but also stable cumene conversion can be achieved over the nanoscale mesoporous aluminosilicates. These results reveal that our nanosized mesoporous aluminosilicates are a capable catalyst of high connectivity and accessibility particularly for large molecules.

Keywords: Nanosized MCM-41; Aluminosilicate; Catalytic cracking

1. Introduction

The discovery of the newest family of mesoporous molecular sieves, designated as the M41S family, is of considerable interest for heterogeneous catalysis [1]. However, their neutral silica frameworks are of limited use for various catalytic applications. The ability to control the chemical composition of these materials is an important topic in catalysis research. Depending on the nature and number of trivalent framework cations, both strength and density of the acid sites can be adjusted to meet the requirements for various processes. For instance, the incorporation of trivalent atoms (Al, Fe, or Ga) into the silica walls creates Brönsted acidic sites and allows the preparation of materials possessing different catalytic and adsorptive properties [2]. Among them, Al-substituted ones have received much attention due to the availability of reagents and the presence of stable and strong active sites [2].

It has been noted that the principal feature of the AlMCM-41 and related solids, namely their ordered unimodal porous structures, does not offer specific advantages in some determined applications, such as in catalysis, especially when bulky molecules are involved [3]. Furthermore, owing to such uniform but long tunnels, unimodal AlMCM-41 could suffer from poor accessibility to active sites and quick deactivation [3]. Indeed, it has been proven that the site accessibility in unimodal MCM-41-like materials can be effectively enhanced by miniaturization of their particle size. It was reported that, for instance, an ultra-small AlHMS catalyst showed a much higher activity for the alkylation of bulky 2,4-di-*tert*-butylphenol with cinnamyl alcohol than typical AlMCM-41 [4], clearly revealing the importance of the ''nano-size'' effect in reactions.

Recently, various types of nanosized mesostructures have been reported [5–15]. However, most of them are only focused on the pure silica species, although the ability to endow nanoparticulate mesostructures with diverse functionalities can increase their application range significantly. This may be associated with the difficult-to-handle conditions (i.e. special techniques) for heteroatom-modified nanosized mesoporous species [8–11,13–15]. Amorós and co-workers reported the

* Corresponding author. Tel.: +82 51 510 2407; fax: +82 51 514 4331.
E-mail address: csha@pusan.ac.kr (C.-S. Ha).

0920-5861/$ – see front matter © 2007 Elsevier B.V. All rights reserved.
doi:10.1016/j.cattod.2007.10.018

preparation of various metal-incorporated MCM-41-like nanocatalysts employing a so-called ''atrane complexing'' method [8–11]; and some of them, as Ti- and V-UVM-7, have been well characterized with excellent performance in olefin epoxidation and selective oxidative activation of isobutane [9,10], respectively. Lin et al. synthesized nanosized AlMCM-41 via a two-step process and the catalyst showed higher activity in cumene cracking than typical AlMCM-41 [13]. Besides, a microwave-hydrothermal route to nanoscale Al-containing mesoporous materials with strong Brönsted acidity has been recently reported [14]. Also, our group reported the synthesis of nanosized mesoporous aluminosilicates with excellent catalytic activity in bulky hydrocarbon cracking reactions, and more desirably, these nanoscale catalysts still displayed high activity even after severe steam treatment [15], which can be mainly attributed to the textural porosity between these aluminosilicated nanoparticles even though the framework structures have been entirely destroyed, clearly revealing the importance of the second porous system in practical applications.

Following previous works on nanoscale mesostructures, we recently developed another more controllable synthesis route to nanosized mesoporous aluminosilicates using a two-step procedure assisted by dual surfactants [16]. For those reported two-step examples, the hydrolysis of silica precursors was inevitably controlled by relatively tedious pH adjustment with additional acids [12,13]; in our case, however, the aluminum salt loaded in the system can promote the hydrolysis of tetraethoxysilane (TEOS) [17], and then nanosized products can be facilely prepared after a fast co-condensation reaction of hydrolyzed species by a basic catalyst. During this process, similar to the role of F127 and FC-4 [12,18], nonionic PEG-4000 could effectively regulate the grain size and distribution through hydrogen-bonding blocking the formed nanocomposites. In the present work, we intend to extend the aforementioned method to characterize typical nanosized mesoporous aluminosilicates with narrow grain size distribution and high Al content and focus on their application as catalyst for the bulky hydrocarbons cracking, which allows us to evaluate the function of highly facilitated porous system in the catalytic performance.

2. Experiment

2.1. Synthesis

Cetyltrimethylammonium bromide (CTAB), aluminum nitrate ($Al(NO_3)_3{\cdot}9H_2O$) and polyethylene glycol (PEG-4000) were purchased from Aldrich. Tetraethoxysilane (TEOS) was supplied from Gelest. All chemicals were used as received.

The principle behind the present synthesis is the independent control of the hydrolysis and condensation of the inorganic precursors, and the synthesis consists of two steps. First, a predetermined amount of CTAB, PEG-4000, TEOS and aluminum salt were mixed and stirred at room temperature for 60 min. Then, a fast co-condensation reaction resulting from the entirely or partly hydrolyzed inorganic species was achieved with the addition of aqueous ammonia, and keeping the pH value of the system at 9–10. After further stirring for 48 h at room temperature, the products were obtained, followed by filtration, drying and calcination. The gel composition can be adjusted within a molar ratio of 1.0TEOS:0.2CTAB:(0.0–0.4)$Al(NO_3)_3$:0.003PEG-4000:200H_2O. Since we have systematically studied the preparative parameters on the structures in the previous works [16], here the emphasis was put on the catalytic characterization of a typical nanosized mesoporous sample prepared with a Si/Al ratio of 5.

2.2. Characterization

Morphology was measured using a scanning electron microscopy (SEM; Jeol JSM 6400) and a transmission electron microscopy (TEM; Tecnai on F20 microscope). X-ray diffraction (XRD) pattern was obtained by using a Rigaku RAD-C system with Cu Kα radiation. N_2 sorption was analyzed on a Micromeritics TriStar 3000 at 77 K. ^{27}Al MAS NMR spectra were obtained on a Bruker DRX 300 spectrometer. Elemental analysis was performed by inductively coupled plasma (ICP) on a Perkin-Elmer 3300 DV. Thermogravimetric analysis (TGA) was carried out on a Perkin-Elmer Pyris Diamond TG instrument at a heating rate of 10 °C/min in air. Temperature programmed desorption of ammonia (TPD-NH_3) was performed in a quartz micro-reactor. 20 mg of sample was heated in argon at 600 °C for 0.5 h. NH_3 was then introduced to the sample after being cooled down to 120 °C. To remove the weakly adsorbed NH_3, the sample was swept using argon at 120 °C for 2 h. Then the TPD experiment was carried out with a carrier-gas flowing rate of 40 mL/min from 120 to 500 °C at 10 °C/min, and the desorption of NH_3 was detected by GC-9A equipped with a TCD detector.

2.3. Catalytic tests

Bulky 1,3,5-triisopropylbenzene (TIPB) and cumene cracking reactions were carried out by conventional pulse method to evaluate catalytic performance of the mesostructured nanoparticles. Typically, 0.2 μL reactant was injected and cracked over 60 mg of catalyst, and nitrogen was used as the carrier gas at a flowing rate of 50 mL/min. The reaction products were analyzed using GC-9A (Shimazu Co.) equipped with a FID detector and a high resolution Chrom-Workstation Data instrument, where online GC was used to determine the reactant conversion.

Blank experiments with substitution of quartz SiO_2 for the catalyst were also tested under the same reaction conditions. No distinguishable thermo-cracking products were observed in these experiments, even at the highest temperature used.

3. Results and discussion

The nanosized mesostructures with a narrow grain size distribution can be clearly identified by SEM and TEM. As shown in Fig. 1(a), the present sample is entirely composed of relatively uniform particles smaller than 100 nm. One should

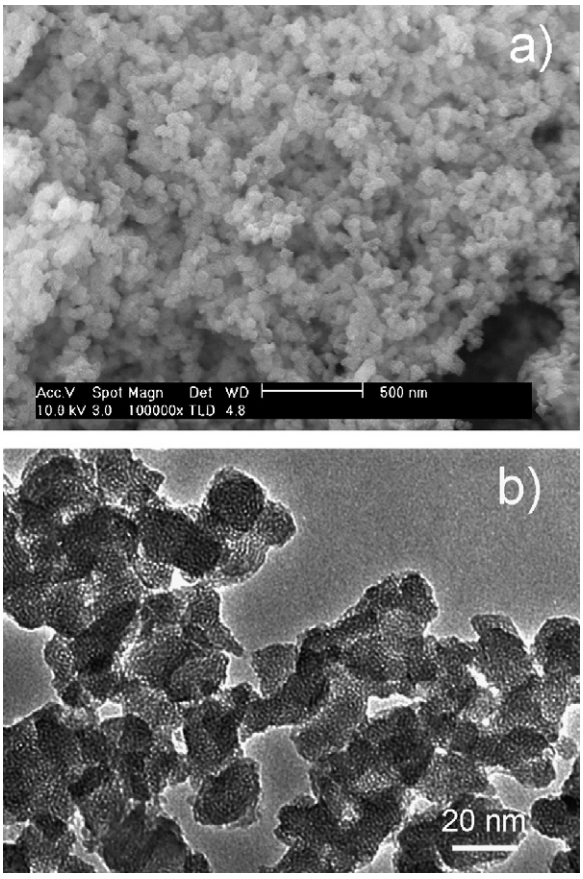

Fig. 1. SEM (a) and TEM (b) images of the typical nanosized aluminosilicates.

note that, however, although there is slight aggregation among the particles, clear and definite edges between these nanoparticles can be seen. The mesoporous structure of these nanoparticles is confirmed by HRTEM (Fig. 1(b)). Relatively uniform pore structures, which have been originated from the cationic micelles, can be clearly observed over the different nanoparticles through the image. However, it should be pointed out that the pore arrangement is not as highly ordered as typical MCM-41 silicas [1,2]. Possibly, the unusual high aluminum content (7.15 wt.%) incorporated in these nanoparticles could be responsible for this phenomenon, similar to those previous observations on nanosized metal-containing mesostructures [8–11]. In contrast to nanosized silicas, the assembly of ordered metal-containing ones is relatively more difficult, and this is likely the reason why some authors employed the ''atrane chelating'' route to synthesize nanosized mesoporous catalysts [8–11,19,20]. Comparatively, the present two-step system assisted by dual surfactants is more effective for the structure control (especially particle size and distribution).

As shown in Fig. 2(a), its XRD pattern shows two distinct peaks, attributable to the (1 0 0) and the overlapped (1 1 0) and (2 0 0) reflections of a MCM-41-type mesostructures, respectively. This pattern is characteristic of slightly distorted hexagonal mesophase, which is well consistent with the above TEM analysis. The porosity of these nanoparticles was further characterized by the N_2 adsorption-desorption isotherm (Fig. 2(b)). Two well-defined steps can be seen in its isotherm. The first one, at intermediate partial pressures ($0.20 < P/P_0 > 0.35$) is due to the capillary condensation of N_2 inside the intra-nanoparticle mesopores. The second step, at a high relative pressure ($P/P_0 > 0.8$), corresponds to the filling of the large inter-particle cage like pores. Even though the XRD pattern in Fig. 2(a) shows somewhat ordered mesopore structure, the N_2 adsorption–desorption isotherm, in particular at intermediate partial pressures ($0.20 < P/P_0 > 0.35$), does not exhibit highly ordered mesopore structure as for the TEM image in Fig. 1(b). As explained above, the result is again due to the presence of unusually high aluminum content in the nanoparticles. The two-step adsorption character is quite similar to that of previously reported nanosized mesostructures [8–17,19–21]. The steepness of both adsorption steps reveals that the intra- and inter-particle pores are quite uniform, which is evidenced by the corresponding pore size distributions (Inset is the intra-particle's but the inter-particle's is not shown here). Besides, this nanosized sample has a specific surface area of

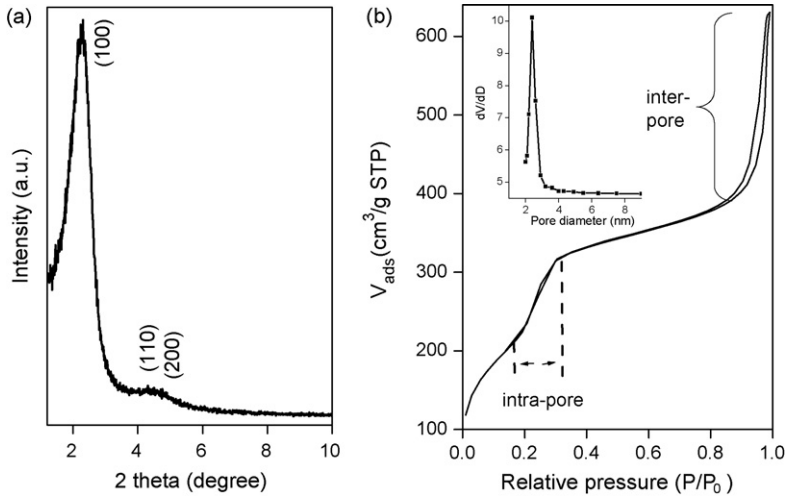

Fig. 2. XRD pattern (a) and N_2 adsorption–desorption isotherm (b) of the nanoscale aluminosilicates (inset, pore size distribution of the framework porosity).

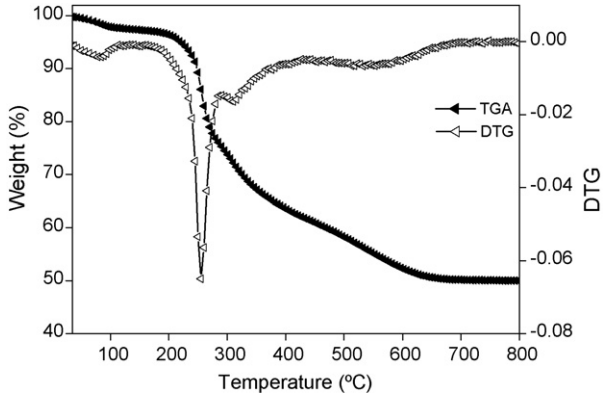

Fig. 3. Thermogravimetric analysis (TGA-DTG) data of the as-synthesized nanosized mesoporous aluminosilicates.

818 m^2/g and a pore volume of 0.91 cm^3/g, which are as high as that for typical MCM-41 silicas.

The thermogravimetric analysis (TGA) data of the as-synthesized mesoporous nanoparticles is illustrated in Fig. 3. Three distinct weight loss stages can be clearly observed. Since the PEG-4000 amount in the synthesis is very small (or can be washed away during the filtration), the weight loss of ca. 40% between 200 and 400 °C can be primarily ascribed to the removal of cationic surfactants occluded in the Al-containing nanoparticles. This high surfactant content indicates that cationic CTAB effectively played the templating function in the assembly process [13,21].

Fig. 4(a) shows the ^{27}Al MAS NMR spectroscopy of the calcined mesoporous nanoparticles with high aluminum content (Si/Al ∼5). Three peaks at 51, 26 and −2 ppm, corresponding to the 4-, 5- and 6-coordinated aluminum species, respectively, can be clearly observed [15,22]. The former is framework aluminum species that locate inside the inorganic porous framework with the Si atoms, whereas the latter two can be assigned to extra-framework aluminum species [22]. The relatively complicated aluminum environment can be attributed to the high Al content in these nanoparticles. Actually, the non-framework Al species reduces considerably or even disappears with increasing Si/Al ratio, which has been evidenced in our previous work [16]. In addition, the extra-framework Al numbers in the nanoparticles can also be effectively reduced by hydrothermal treatment [16].

As one of the major applications of Al-containing materials is used as solid acids, characterization of the acidity, therefore, is very important. Fig. 4(b) shows the TPD-NH_3 profile of the present nanosized aluminosilicates. Interestingly, two desorption peaks at ca. 210 and 305 °C can be distinctly observed. Both strong signals reveal that the acidic site amount on these nanoparticles is quite large and easily accessible to probe molecules. Almost all adsorbed ammonia molecules can be desorbed above 480 °C, corresponding to the acidic sites with medium strength and well consistent with the previous results on mesoporous aluminosilicates [2,23]. It is desirable that, since no alkali metals (e.g. K^+, Na^+) present in the synthesis system, some time-consuming post-treatments such as ion-exchange and activation can be avoided. Hence, nanoscale acidic catalysts with high density of active centers can be directly obtained just after the removal of surfactants by calcination, which is one of the advantages of the present synthesis.

It has been well demonstrated that microporous zeolites (ZSM-5, Y, Beta, etc.) cannot sufficiently catalyze the cracking of bulky alkyl aromatic TIPB (kinetic diameter ca. 0.94 nm) due to the geometrical restrictions to their dominant internal active centers; and therefore only very small amount of TIPB can be cracked on the external surface of zeolite crystals [24], albeit they have much stronger acidity. In contrast, taking advantages of tunable mesopores and suitable acidity, mesostructured aluminosilicates are promising catalyst candidates for catalytic cracking of long-chain hydrocarbons, particularly of the petroleum residues for which high reaction temperatures are favorable. Therefore, TIPB cracking reactions have been tested over these mesoporous Al-containing

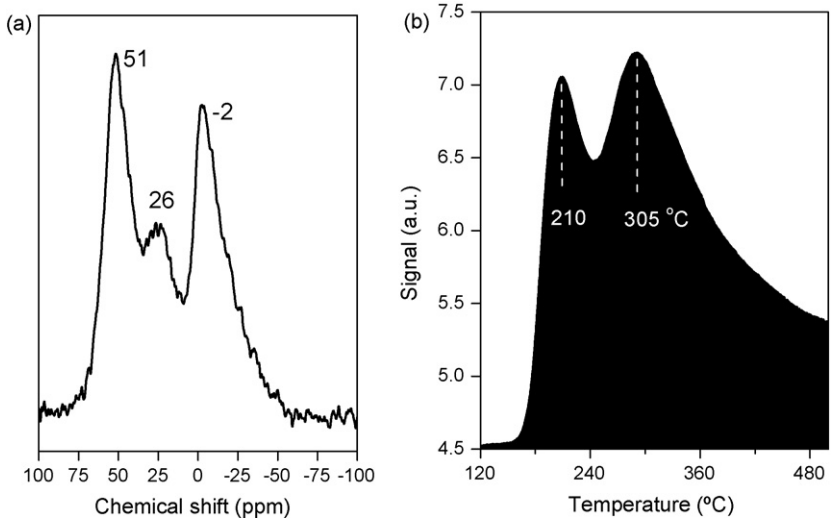

Fig. 4. Solid state ^{27}Al MAS NMR spectrum (a) and TPD-NH_3 profile (b) of the nanosized aluminosilicates.

Table 1
Catalytic results of TIPB cracking over the nanocatalyst at various temperatures

Tempearture (°C)	Conversion (mol%)	Selectivity				
		Propene	Benzene	Isopropylbenzene	*m*-D[a]	*p*-D[a]
250	100	41.65	5.01	46.38	4.93	1.99
280	100	46.95	7.77	44.20	1.05	–[b]
300	100	47.97	11.23	39.83	–	–
310	100	49.42	13.99	35.88	–	–
340	100	52.54	20.86	25.77	–	–

Conversions were taken at the fifth pulse.
[a] Stands for *m*-diisopropylbenzene and *p*-diisopropylbenzene, respectively.
[b] Product undetectable.

nanoparticles at various temperatures, and the catalytic results are shown in Table 1. Noticeably, the present nanoscale meso-catalyst is very active toward this reaction, large TIPB can be completely cracked even at the lowest temperature of 250 °C, and this may be closely associated with its facilitated pore system and high density of acidic sites [13–15]. More interestingly, the selectivity varies greatly with the reaction temperature. In all cases, the steadily increased selectivity to propylene and benzene and significantly opposite changes for isopropyl benzene (IPB) and diisopropyl benzene (DIPB) can be seen clearly, meaning the total conversion (including TIPB, IPB and DIPB) increases considerably with the reaction temperatures. Similar trend in selectivity evolution with temperature was also observed for the previous catalysts [15]. However, one should note that, even though the selectivity to IPB always decreases with temperature, it is still one of the main products in the whole process. This indicates that, not like DIPB, IPB cannot be entirely cracked over the present nanosized alumniosilicates. To better understand the catalytic behavior of the present catalyst in IPB cracking, it is useful to carry out the experiment using pure IPB as the model reactant, which is also usually used to characterize mesoporous solid acids [24,25].

Different from bulky TIPB cracking, which requires weak and moderate acidity, the cracking of relatively small cumene needs a catalyst with medium and strong acidic centers [24,25]. The cumene cracking over these moderately acidic nanoparticles was tested at 300 °C, propene and benzene are the major products of this reaction. In addition, similar to previous results, minor alkylation species such as DIPB can also be detected [24,25]. Fig. 5 shows the dependence of cumene cracking conversion on the pulse times. Generally, the catalytic activities decrease remarkably with pulse number, as reported for typical AlMSU-x, AlMCM-41 and SO_4^{2-}/ZrO_2/MCM-41 catalysts [24,25]. In contrast, the current bimodal aluminosilicates exhibited a stable catalytic activity toward cumene cracking. The conversion is still over 45% even at the 30th time (the process is about 14 h). These results suggest that the sample has good catalytic durability, and this can be attributed to its highly accessible acidic sites and diffusion-facilitated framework [9,13,15]. As compared to the industrially zeolitic cracking catalysts, however, the present catalyst is not extraordinarily active in this reaction, which is well consistent with its moderate acidity in nature [2]. However, taking its bimodal mesopores and comparable acidity into account, we can see that the sample has a bright future in the transformation of relatively larger molecules, especially when high-reaction temperatures are demanded.

These catalytic features, similar to those observed with AlMCM-41, could be expected because of their similar acidic properties and structural features. Indeed, the present sample can be considered as a kind of nanosized AlMCM-41. In this structure the mesopores are unidirectional, parallel and not interconnected. Hence, the mesopore channel length is equal to the particle length along the *x*-axis, namely, micrometric for AlMCM-41 and nanometer-sized for the present sample. Therefore, by comparing the catalytic performance of these two types of materials with similar Si/Al ratios, one may get information on the influence of channel length and the average residence time inside the channel on the catalytic behavior, particularly for bulky molecules. Actually, relative to typical AlMCM-41, the improvement of the catalytic activity in several condensed phase reactions (cracking and alkylation reactions) and the acidity duration to severe steam regeneration conditions of nanosized mesoporous aluminosilicates has been well demonstrated in our previous work [15,26]. This implies that, besides the nature of the aluminum centers and pore structures, the macroscopic morphology (i.e. particle size) also plays important role in the practical processes, supporting those earlier proposals [3,8–10,13].

Before concluding, it should be noted here that further work is necessary to reveal systematically the relationship of the acidity and catalytic activity as well as the exact information of

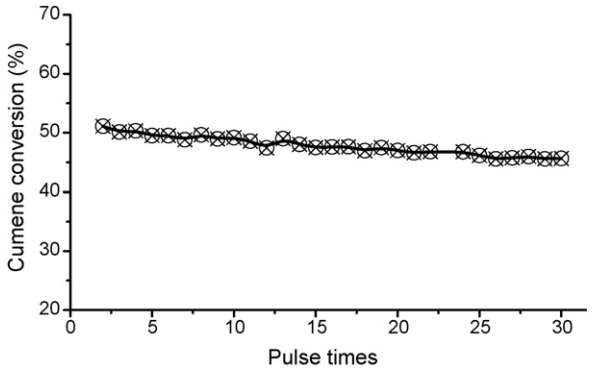

Fig. 5. The dependence of cumene conversion on the pulse times over the nanosized catalyst.

acidic nature (acidic sites) of the present mesoporous aluminosilicate nanoparticle system. Moreover, the measurement of the catalytic activity under steady-state reaction conditions should be done since the catalytic durability cannot be explained only by the pulsing method under the unsteady-state conditions. Further works on these subjects are now underway and will be reported elsewhere.

4. Conclusions

The novel two-step route assisted with dual surfactants allows preparing narrowly-distributed mesoporous Al-containing nanoparticles without considerable loss of the hexagonal order for Al content up to Si/Al $\geq$ 5. This nanoscale catalyst constituted a high density of acidic sites and diffusion-eased bimodal pore system, which can benefit to the improvement of the catalytic efficiency in the transformation of bulky hydrocarbons.

Acknowledgements

This study was financially supported by the Pusan National University in the Program, Post-doc. 2006 (for S.R.Z.), the Korea Science and Engineering Foundation (KOSEF) through the National Research Laboratory Program funded by the Ministry of Science and Technology (MOST; M10300000369-06J0000-36910), the SRC/ERC Program of MOST/KOSEF (grant #R11-2000-070-080020) and the Brain Korea 21 Project.

References

[1] C.T. Kresge, M.E. Leonowicz, W.J. Roth, J.C. Vatuli, J.S. Beck, Nature 359 (1992) 710.
[2] A. Corma, Chem. Rev. 97 (1997) 2373.
[3] D.R. Rolison, Science 299 (2003) 1698.
[4] T.R. Pauly, Y. Liu, T.J. Pinnavaia, S.J. Billinge, T.P. Rieker, J. Am. Chem. Soc. 121 (1999) 8835.
[5] Q. Cai, Z.S. Luo, W.Q. Pang, Y.W. Fan, X.H. Chen, F.Z. Cui, Chem. Mater. 13 (2001) 258.
[6] R.I. Nooney, D. Thirunavukkarasu, Y. Chen, R. Josephs, A.E. Ostafin, Chem. Mater. 14 (2002) 4721.
[7] S. Sadasivan, C.E. Fowler, D. Khushalani, S. Mann, Angew. Chem. Int. Ed. 41 (2002) 2151.
[8] J.E. Haskouri, D.O. de Zárate, C. Guillem, J. Latorre, M. Caldés, A. Beltrán, D. Beltrán, A.B. Desscalzo, G.R. López, R.M. Máñez, M.D. Marcos, P. Amorós, Chem. Commun. (2002) 330.
[9] J.E. Haskouri, D.O. de Zárate, F. Pérez-Pla, A. Cervilla, C. Guillem, J. Latorre, M.D. Marcos, A. Beltran, D. Beltrán, P. Amorós, New J. Chem. 26 (2002) 1093.
[10] L.J. Huerta, P. Amorós, D. Beltrán-Porter, V. Cortés Corberán, Catal. Today 117 (2006) 180.
[11] D.O. de Zárate, A. Gómez-Moratalla, C. Guillem, A. Beltrán, J. Latorre, D. Beltrán, P. Amorós, Eur. J. Inorg. Chem. 13 (2006) 2572.
[12] K. Suzuki, K. Ikari, H. Imai, J. Am. Chem. Soc. 126 (2004) 462.
[13] M. Chao, H. Lin, C. Mou, B. Cheng, C. Cheng, Catal. Today 97 (2004) 81.
[14] C.F. Cheng, H.H. Cheng, L.L. Wu, B.W. Cheng, Stud. Sci. Surf. Catal. 156 (2005) 113.
[15] S.R. Zhai, Y. Zhang, D. Wu, Y.H. Sun, S.J. Wang, Top. Catal. 39 (2006) 227.
[16] S.R. Zhai, C.S. Ha, Micropor. Mesopor. Mater. 102 (2007) 212.
[17] S.Y. Chen, L.Y. Jang, S. Cheng, Chem. Mater. 16 (2004) 4174.
[18] Y. Han, J.Y. Ying, Angew. Chem. Int. Ed. 44 (2005) 288.
[19] J.M. Marales, J. Latorre, C. Guillem, A. Beltrán-Porter, D. Beltrán-Porter, P. Amorós, Solid State Sci. 7 (2005) 415.
[20] L.J. Huerta, C. Guillem, J. Latorre, A. Beltrán, R. Martínez-Máñez, M.D. Marcos, D. Beltrán, P. Amorós, Solid State Sci. 8 (2006) 940.
[21] H.P. Lin, C.P. Tsai, Chem. Lett. 32 (2003) 1092.
[22] Y. Li, Q.H. Yang, J. Yang, C. Li, J. Porous Mater. 13 (2006) 187.
[23] E.F.S. Aguiar, M.L. MurtaValle, M.P. Silva, D.F. Silva, Zeolites 15 (1995) 620.
[24] L. Zhu, F.S. Xiao, Z.T. Zhang, Y.Y. Sun, Y. Han, S.L. Qiu, Catal. Today 68 (2001) 209.
[25] Y.Y. Sun, L. Zhu, H.J. Lu, R.W. Wang, D.Z. Jiang, F.S. Xiao, Appl. Catal. A: Gen. 237 (2002) 21.
[26] S.R. Zhai, C.S. Ha, Y. Liu, H.Y. Qiu, D. Wu, Y.H. Sun, S.J. Wang, B. Zhai, Stud. Surf. Sci. Catal. 165 (2007) 807.